Huffman Sequence Design for Coded Excitation in Medical Ultrasound

Alessandro Polpetta, Paolo Banelli
Electronic and Information Engineering Department (DIEI)
University of Perugia, Italy

Abstract

This paper deals with the design of coded-excitation signal for medical ultrasound imaging. In order to design a code sequence that generates an ultrasound signal with good detail resolution and signal-to-noise ratio, both in frequency-dependent and frequency-independent attenuating media, we propose to use a linear Huffman code obtained by an efficiency-driven optimizing procedure. By resorting to computer simulations, we show that this approach is particularly effective and it outperforms other linear coding schemes commonly used in coded-excitation ultrasound imaging.

1. Introduction

Ultrasound coding excitation (CE) in medical imaging is a transmission technique that allows to increase the transmitted energy without increasing the pulse amplitude [1]–[5], by exciting the ultrasound transducer with a long modulated pulse characterized by a Time-Bandwidth-Product greater than one. In the CE framework, some authors proposed single [3] and double transmissions [4] with binary-coded modulations, which are characterized by extremely low complexity. For instance, complementary Golay codes [4], thanks to the side-lobes cancellation granted by double transmissions, provide ideal performance in frequency flat environments, although they highly suffer the presence of frequency-dependent attenuations [2]. On the contrary, linear-FM codes [2] (i.e. chirp) are robust against frequency-dependent attenuations, but suffer of a non-ideal autocorrelation function and, thus, of a worse contrast resolution. In order to have a CE technique characterized by quasi-ideal performance, both in the absence and in the presence of frequency-dependent attenuations, we propose to code the signal by resorting to Huffman sequences, which combine amplitude with phase (and thus frequency) modulation.

To this end, Section 2 provides details of a typical CE architecture, while Section 3 briefly summarizes the Huffman coding theory. Section 4 tests the proposed Huffman coding approach by means of typical ultrasound performance indexes, also employing the Field II [6] simulator, and it makes comparisons with double-transmission Golay CE [4] and with a single-transmission binary CE that employs inverse filtering [3].

2. System Architecture and Ultrasound Coding Excitation

Fig. 1 describes the TX/RX block diagram of a CE ultrasound system that employs a phased-array probe with Q piezoelectric elements.

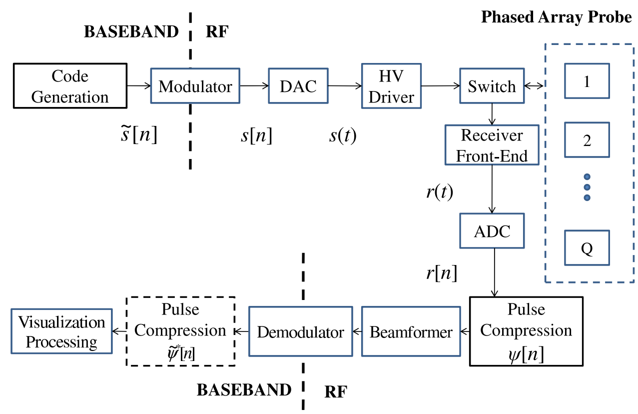

Figure 1. Block diagram of a coded-excitation ultrasound system.

The code generator produces the discrete-time baseband digital signal $\tilde{s}[n]$ that is modulated to obtain the RF signal $s[n]$ expressed by

$$s[n] = \Re\{\tilde{s}[n]e^{j2\pi f_0 T_s n}\}, \tag{1}$$

where f_0 is the ultrasound center frequency and $T_s = 1/f_s$ is the sampling generation time. After digital-to-analog conversion (DAC) and proper amplification, the signal $s(t)$ excites the ultrasound piezoelectric elements.
At the receiver side, in the case of a single scatterer and ignoring noise and signal attenuation, the analog-to-digital converter (ADC) output $r[n]$ can be approximated by the time- and frequency-shifted version of the transmitted signal $s[n]$, as expressed by

$$r[n] \approx \Re\{\tilde{s}[n-k_0]e^{j2\pi[-f_d(n-k_0)T_s]}\}, \tag{2}$$

where k_0 is the digital round trip delay, f_d is the frequency shift induced by the frequency-dependent attenuation [1], and T_s is the sampling interval that, for simplicity, is assumed equal to that one used in the generation process. The frequency shift is typically approximated by [7]

$$f_d = \beta B_r^2 f_0^2 z, \tag{3}$$

where β is the frequency dependent attenuation coefficient, B_r is the relative bandwidth of the transmitted pulse and z is the depth of the reflecting scatterer.

The discrete-time RF signal $r[n]$ is successively processed to compress (decode) the effective impulse response, and consequently restore the spatial resolution. More precisely, the output of the pulse compressor is obtained by cross-correlating the received waveform $r[n]$ with the pulse compression waveform $\psi[n]$, as expressed by

$$R_{r\psi}[k] \quad = \quad \sum_{m=-\infty}^{+\infty} r[m]\psi[k+m], \tag{4}$$

which is summarized by its baseband complex counterpart $\widetilde{R}_{\widetilde{r}\widetilde{\psi}}[k]$ expressed by

$$\widetilde{R}_{\widetilde{r}\widetilde{\psi}}[k] = \sum_{m=-\infty}^{+\infty} \widetilde{r}^*[m]\widetilde{\psi}[k+m], \tag{5}$$

and where, by means of (1), $\widetilde{r}[n]$ and $\widetilde{\psi}[n]$ are the complex envelope associated to the RF received signal $r[n]$ and the compression waveform $\psi[n]$, respectively. While in the absence of frequency-dependent attenuation the pulse compression output is $\tilde{R}_{\tilde{r}\tilde{\psi}}[k] \approx \tilde{R}_{\tilde{s}\tilde{\psi}}[k+k_0]$, when $f_d \neq 0$ (5) becomes $\tilde{R}_{\tilde{r}\tilde{\psi}}[k] \approx \widetilde{\chi}_{\widetilde{s}\widetilde{\psi}}(k+k_0, f_d)$, where the ambiguity function

$$\widetilde{\chi}_{\widetilde{s}\widetilde{\psi}}(k, f_d) = \sum_{m=-\infty}^{+\infty} \widetilde{s}^*[m]\widetilde{\psi}[m+k]e^{-j2\pi f_d m T_s} \tag{6}$$

shows how the cross-correlation function changes with a frequency variation f_d.

Our aim is to design a system characterized by a ridge [1] ambiguity function, in order to guarantee, even with a frequency-dependent attenuation, both a good detail and a good contrast resolution, which depend, respectively, on the width of the main lobe and on the ratio MSR between the main lobe and the side lobes of $|\widetilde{R}_{\widetilde{r}\widetilde{\psi}}[k]|$. When the compression waveform $\psi[n]$ is equal to the transmitted signal $s[n]$, the pulse compression is the classical matched filter and thus we would have $\widetilde{R}_{\widetilde{r}\widetilde{\psi}}[n] = \widetilde{R}_{\widetilde{r}\widetilde{s}}[n] \approx \widetilde{\chi}_{\widetilde{s}\widetilde{s}}(k+k_0, f_d)$. Moreover, we want to compare the obtained CE performance with those of other linear codes (L)-CEs that are generally expressed by the baseband signal

$$\widetilde{s}[n] = \sum_{i=0}^{N} c_i p[n-iM], \tag{7}$$

where $p[n]$ is the pulse shaping waveform, c_i are the codes of length N, and M is an opportune upsampling factor.

We will compare different (L)-CE approaches with respect to the detail and the contrast resolution, and the signal-to-noise ratio gain $GSNR$, which is defined by

$$GSNR = \frac{SNR_c}{SNR_0} = \frac{|R_{r\psi}[0]|^2}{(|R_{\psi\psi}[0]|\sigma^2)} \cdot \frac{|R_{s_0 s_0}[0]|\sigma^2}{|R_{r_0 s_0}[0]|^2}, \tag{8}$$

where σ^2 is the system noise power, SNR_c is the signal-to-noise ratio guaranteed by the CE technique and a pulse compression waveform $\psi[n]$, and SNR_0 is the SNR at the reception of $r_0[n]$ when a single pulse (without CE) $s_0[n] = p[n]\sin[2\pi f_0 n]$ is transmitted.

3. Huffman coding

The design of good linear CE sequences aims at obtaining a coded waveform $s[n]$ characterized by an autocorrelation function $\widetilde{R}_{\widetilde{s}\widetilde{s}}[k]$ that is similar to that one of a single strong pulse, and, in the presence of frequency shifts, a ridge ambiguity function. Thus, by means of eq. (7) our goal is to find a sequence $\{c_i\}$ whose discrete autocorrelation function is similar to a Kronecker delta ($R_{cc}[k] = \sum_{i=0}^{N-k} c_i c_{i+k}^* = \delta[k]$) such that $\widetilde{R}_{\widetilde{s}\widetilde{s}}[k] = R_{pp}[k]$, and successively to design $p[n]$ in order to meet our requirements.

In 1962 Huffman [8] found out a family of complex discrete sequences $\{c_{Hi}\}$ with autocorrelation functions $R_{c_H c_H}[k]$ expressed by

$$R_{c_H c_H}[k] = \begin{cases} \sum_{i=0}^{N} |c_{H,i}|^2, & k = 0 \\ 0, & 0 < k < N \\ -\dfrac{R_{c_H c_H}[0] X^{-N}}{1 - X^{-2N}}, & k = N \end{cases}, \tag{9}$$

where X is a design parameter, and that, by means of (9), are close to our desired target, except for $k = N$. Huffman demonstrated that a sequence $\{c_i\}$ has the autocorrelation function expressed by (9) if its Z-transform $C_H(z)$

$$\begin{aligned} C_H(z) &= c_{H,0} + c_{H,1} z^{-1} + \ldots + c_{H,N} z^{-N} \\ &= c_{H,0} \prod_{i=1}^{N} (1 - z^{-1} z_i), \end{aligned} \tag{10}$$

has all the zeros z_i that are spaced at equal angular intervals in the z-plane and lie in one of two origin-centered circles, with radius X and $1/X$, as expressed by

$$z_i = \begin{cases} X e^{j2\pi i/N}, & \text{if the } i\text{th zero has radius } X \\ X^{-1} e^{j2\pi i/N}, & \text{if the } i\text{th zero has radius } 1/X \end{cases}. \tag{11}$$

Further properties of this kind of sequences can be summarized as

$$\begin{aligned} MSR = R_{c_H c_H}[0] = X^N + X^{-N} \\ \eta = \frac{MSR}{\max_n |c_{H,n}|^2} \end{aligned}, \tag{12}$$

where the MSR is equal to the code energy, and η represents the efficiency of the sequence, which influences the $GSNR$ achievable with the specific code.

Once the two parameters N and X are selected (e.g. by choosing the maximum sequence length and the MSR in (12)), according to (10), there are 2^N different sequences with the same autocorrelation function expressed by (9), each one characterized by its own efficiency η and ambiguity function $\widetilde{\chi}_{\widetilde{s}\widetilde{s}}(k, f_d)$. We suggest to apply the synthesizing method described by Ackroyd in [9] in order to choose the Huffman sequence $\{c_{Hi}\}$. Indeed, although this procedure consists on the search of the Huffman zero pattern that maximize the code efficiency η in (12), it also provides a sequence with a very ridge ambiguity function.

4. Coding Performance

In this section we compare the performance of the proposed Huffman sequence design with two other linear coding approaches described in [3] and [4]. First we evaluate the matched and mismatched filter output for the different coding methods. Successively, by exploiting the Field II simulator [6], we compare the scan-lines amplitudes obtained with a B-mode imaging approach and a specific beamforming scheme, taking into account also the tissue attenuation (e.g. the ambiguity function impact).

We consider a linear code length $N = 26$ and a pulse shaping waveform $p[n]$ designed as a 120 taps FIR filter with $B = 2.6$ MHz that implements the Gaussian ($\alpha = 3.5$) window described in [10], whose pulse compression performance are better evaluated in [11]. The up-sampling factor has been set to $M = \lceil f_s/B \rfloor = 38$, which corresponds to a signal duration $T \approx 10\mu s$ at $f_s = 100$ MHz.

The Huffman sequence has been generated according to the Ackroyd approach [9], by setting in (12) the parameter X in order to guarantee $MSR = 100$ dB.

For a first comparison we use the binary inverse filtering (BIF) code sequence found in [3] with $N = 26$. This is the ”near optimal sequence” and a FIR least square inverse filter is employed as pulse compression mismatched filtering. We use a filter code length $N_\psi = 3N$, as suggested in [3].

An alternative linear CE is the Golay coding approach described in [4], which provides ideal impulse-like autocorrelation performance at the price of a double transmission and, consequently, of a frame-rate reduction in B-mode images. Additionally, motion artifacts are expected to degrade the side-lobe cancellation.

The performance are evaluated when the received signal is altered by the presence of a transducer impulse response. More precisely we consider a 4 MHz transducer with 65% of fractional bandwidth, modeled as a linear band-pass filter implemented as a two stage 101 taps FIR filter that employs Hamming windowing.

Fig. 2 compares the matched filter output $\widetilde{R}_{\widetilde{r}_H \widetilde{s}_H}[k]$ of the Huffman sequence, versus the mismatched filter output of a binary sequence with inverse filtering designed as [3] and versus a double transmission Golay matched filter as in [4],

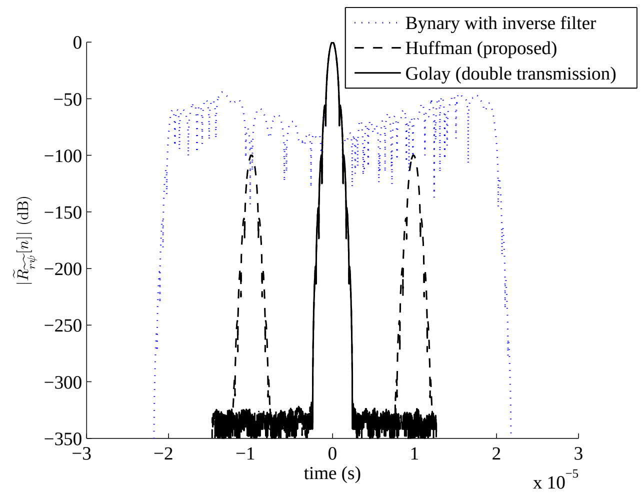

Figure 2. Pulse compression performance comparison in absence of frequency-dependent attenuation.

in the absence of frequency-dependent attenuation. It is clear that, in this scenario, the Golay approach provides ideal MSR performance, the inverse filtering method guarantees $MSR \approx 45$ dB, while the Huffman coding is designed in order to have $MSR = 100$ dB. The main lobe, and thus the axial resolution, of all the three methods is identical. Indeed it can be easily demonstrated that for linear coding the main-lobe amplitude depends only on the pulse shaping function $p[n]$ that is used (see [11] for further details).

Table 1. Performance comparison of Huffman, (BIF) [3] and Golay [4] codes in frequency-flat media.

	Huffman	BIF [3]	Golay [4]
$GSNR$ (dB)	9.3	8.9	13.6
MSR (dB)	100	45	∞
Axial Resolution (mm)	1.7	1.7	1.7

Table 1 shows that, as concern the $GSNR$ performance, the Huffman code largely outperforms the single transmission (BIF) described in [3], while the Golay code [4], also thanks to its double transmission, provides significantly higher values of $GSNR$.

Fig. 2 and Table 1 suggest that, in the absence of frequency-dependent attenuation, the Golay approach outperform the others at the price of a reduction of the B-mode frame-rate. In order to better judge the coding performance in a realistic scenario, we evaluate also the pulse compression output in the presence of a frequency-dependent attenuating medium ($(\beta)_{\mathrm{dB}} = 0.7\mathrm{dB}/(\mathrm{MHz}\cdot\mathrm{cm})$) and also considering a beamforming technique. More precisely we ran ultrasound imaging simulations by exploiting Field II [6] to model the probe, the frequency-dependent tissue as well as the impact of the beamforming. We fixed 8 points scatterers along the axial direction, spaced 20 mm from each other, at absolute distances ranging from 40 to 200 mm from the transducer, which is modeled as a 32 elements phased array probe. We also used a fixed focus transmission beamforming [12] at 100 mm distance and a dynamic receive beamforming [12]. As we did for the results of Fig. 2, each piezoelectric element is modeled by a filter with center nominal frequency $f_0 = 4$ MHz and with 65% fractional bandwidth.

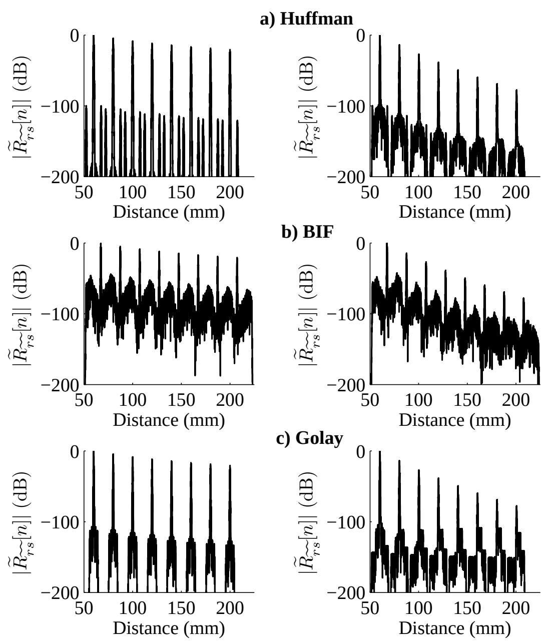

Figure 3. Compressed central rf-line in frequency-independent (left) and frequency-dependent attenuating medium (right) for a) Huffman coding (top) - b) BIF coding (middle) - c) Golay coding (bottom).

Fig. 3 (a)-(c) show the compressed RF-line in a frequency-independent and in frequency-dependent mediums ($\beta = 0.7\mathrm{dB}/(\mathrm{MHz}\cdot\mathrm{cm})$) for Huffman, BIF and Golay coding, respectively. It is now evident that, in the presence of attenuation, both the BIF and the Golay coding suffer a pronounced degrade of MSR, especially for far scatterers. On the contrary, thanks to the quasi-ridge ambiguity function of the design we propose, Huffman coding provides very good performance also in the presence of frequency-dependent attenuation, thus outperforming the other linear CE approaches in practical scenarios.

5. Conclusions

This paper has presented a new approach for linear coding excitation in medical ultrasound systems, based on Huffman coding theory. The transmitted Huffman sequence is designed by a technique that, for a fixed code length, optimizes the code efficiency and thus the final $GSNR$ and that also provides a very good ambiguity function to ensure robustness of the system against frequency-dependent tissue attenuations. Pulse compression is performed by a matched filtering approach and provides a very good contrast resolution if compared with single [3] and double transmission [4] coding, especially in attenuating tissues.

References

[1] T. Misaridis and JA Jensen. Use of modulated excitation signals in medical ultrasound. Part I: basic concepts and expected benefits. *IEEE Transactions on Ultrasonics, Ferroelectrics and Frequency Control*, 52(2):177–191, 2005.

[2] T. Misaridis and JA Jensen. Use of modulated excitation signals in medical ultrasound. Part II: design and performance for medical imaging applications. *IEEE Transactions on Ultrasonics, Ferroelectrics and Frequency Control*, 52(2):192–207, 2005.

[3] K. Liu and S. Gao. Searching binary sequences for coded excitation in medical ultrasound. In *27th Annual International Conference of the Engineering in Medicine and Biology Society, 2005*, pages 1858–1860, 2005.

[4] RY Chiao and LJ Thomas. Synthetic transmit aperture imaging using orthogonal Golay coded excitation. In *2000 IEEE Ultrasonics Symposium*, volume 2, 2000.

[5] JA Jensen et al. Ultrasound research scanner for real-time synthetic aperture data acquisition. *IEEE Transactions on Ultrasonics, Ferroelectrics and Frequency Control*, 52(5):881–891, 2005.

[6] J.A. Jensen. Field: A program for simulating ultrasound systems. *Medical and Biological Engineering and Computing*, 34:351–352, 1996.

[7] J.A. Jensen. *Estimation of blood velocities using ultrasound: a signal processing approach*. Cambridge University Press, 1996.

[8] D. Huffman. The generation of impulse-equivalent pulse trains. *IRE Transactions on Information Theory*, 8(5):10–16, 1962.

[9] MH Ackroyd. Synthesis of efficient Huffman sequences. *IEEE Transactions on Aerospace and Electronic Systems*, pages 2–8, 1972.

[10] JW Adams. A new optimal window [signal processing]. *IEEE Transactions on signal processing*, 39(8):1753–1769, 1991.

[11] A. Polpetta and P. Banelli. Design and Performance Evaluation of Huffman Sequences for Medical Ultrasound Coding Excitation. *submitted to IEEE Transactions on Ultrasonics, Ferroelectrics and Frequency Control*.

[12] B.D. Steinberg. Digital beamforming in ultrasound. *IEEE Transactions on Ultrasonics, Ferroelectrics, and Frequency Control*, 39(6):716–721, 1992.